



Glial Fibrillary Acidic Protein and Ionized Calcium-Binding Adapter Molecule 1 Immunostaining Score for the Central Nervous System of Horses With Non-suppurative Encephalitis and Encephalopathies

Gisele Silva Boos^{1*}, Klaus Failing², Edson Moleta Colodel³, David Driemeier⁴, Márcio Botelho de Castro⁵, Daniele Mariath Bassuino⁶, José Diomedes Barbosa⁷ and Christiane Herden¹

OPEN ACCESS

Edited by:

Enric Vidal,
IRTA-CReSA, Centre for Research on
Animal Health, Spain

Reviewed by:

Daniel Emy,
University of Freiburg Medical
Center, Germany
Ana Alba Casals,
Institute of Agrifood Research and
Technology (IRTA), Spain
Marta Monzon,
University of Zaragoza, Spain

*Correspondence:

Gisele Silva Boos
gisele.s.boos@vetmed.uni-giessen.de

Specialty section:

This article was submitted to
Veterinary Experimental and
Diagnostic Pathology,
a section of the journal
Frontiers in Veterinary Science

Received: 28 January 2021

Accepted: 08 June 2021

Published: 09 July 2021

Citation:

Boos GS, Failing K, Colodel EM,
Driemeier D, Castro MBd,
Bassuino DM, Diomedes Barbosa J
and Herden C (2021) Glial Fibrillary
Acidic Protein and Ionized
Calcium-Binding Adapter Molecule 1
Immunostaining Score for the Central
Nervous System of Horses With
Non-suppurative Encephalitis and
Encephalopathies.
Front. Vet. Sci. 8:660022.
doi: 10.3389/fvets.2021.660022

¹ Department of Veterinary Medicine, Institute of Veterinary Pathology, Justus-Liebig-Universität, Gießen, Germany, ² Unit of Biomathematics and Data Processing, Department of Veterinary Medicine, Justus-Liebig-Universität, Gießen, Germany, ³ Laboratory of Veterinary Pathology, Universidade Federal do Mato Grosso, Cuiabá, Brazil, ⁴ Department of Veterinary Pathology, Universidade Federal do Rio Grande do Sul, Porto Alegre, Brazil, ⁵ Laboratory of Veterinary Pathology, Universidade de Brasília, Brasília, Brazil, ⁶ Laboratory of Veterinary Pathology, Universidade de Cruz Alta, Cruz Alta, Brazil, ⁷ Veterinary Diagnostics Center, Veterinary Institute, Universidade Federal do Pará, Castanhal, Brazil

Like humans, horses are susceptible to neurotropic and neuroinvasive pathogens that are not always readily identified in histological sections. Instead, alterations in astrocytes and microglia cells can be used as pathological hallmarks of injured nervous tissue in a variety of infectious and degenerative diseases. On the other hand, equine glial cell alterations are poorly characterized in diseases. Therefore, in this study, we provide a statistically proved score system to classify astrogliosis and microgliosis in the central nervous system (CNS) of horses, based on morphological and quantitative analyses of 35 equine cases of encephalitis and/or encephalopathies and four non-altered CNS as controls. For this system, we used glial fibrillary acidic protein (GFAP) and ionized calcium-binding adapter molecule 1 (Iba1) immunohistochemistry, allied to statistical analysis to confirm that the scores were correctly designated. The scores of alterations ranged from 0 (non-altered) to 3 (severely altered) and provided a helpful method for describing astrocytic and microglial alterations in horses suffering from inflammatory and degenerative lesions. This system could be a template for comparative studies in other animal species and could aid algorithms designed for artificial intelligence methods lacking a defined morphological pattern.

Keywords: astrocytes, microglia, score system, etiology, infectious, degenerative

INTRODUCTION

Astrogliosis and microgliosis have been used as pathological hallmarks of injured nervous tissue in a variety of degenerative and infectious diseases (1–7). Analyses of features like quantitative and morphological alterations of astrocytes and microglia cells are commonly carried out after immunohistochemistry (IHC) employing antibodies directed against the glial fibrillary acidic

protein (GFAP) and the ionized calcium-binding adapter molecule 1 (Iba1) (5, 8–11). Additionally, improvements in glial quantification techniques, also applied with these markers, through machine learning algorithms have shown a marked reduction in analysis time, increased productivity, and comparable accuracy as with manual techniques (12, 13). Astrocytic and microglial alterations have been more closely documented in neurodegenerative diseases in humans and experimental animal models, but little information is available on glial alterations in the central nervous system (CNS) of horses (14, 15). As equines are similarly susceptible to several neuroinvasive pathogens as humans (e.g., Borna disease virus, West Nile virus, and rabies virus) and might display degenerative/traumatic conditions that could mimic an infection, horses are valuable models for risk assessment of zoonoses and differential diagnosis (2, 16–20).

The establishment of a reliable quantitative and morphological classification system of astrocytic and microglial alterations in horses can help address lesion patterns on unresolved cases of encephalitis and encephalopathies. Pathologists could use the system for a complimentary assessment of lesions in the CNS and comparative studies involving glial response to injury by pathogens and/or degenerative lesions also in other animal species and humans. Meanwhile, an established score system for glial alterations would also benefit machine learning systems, as it would provide a morphological template of different stages of alterations to complement algorithms for automatic quantification.

In this light, this study aimed to establish score systems for GFAP and Iba1 immunostaining for the CNS of horses, considering the morphology and the number of astrocytes and microglia cells stained using natural cases of inflammation and degenerative lesions as a template.

MATERIALS AND METHODS

Samples

To demonstrate the spectrum of astrocytic and microglial alterations, there were 39 CNS sections from horses available for the study. Samples were selected among necropsy cases that remained with an unclear etiologic diagnosis from horses with neurological clinical signs that do not rule out an infectious cause. These samples comprised 28 cases with inflammatory lesions suggested and/or confirmed to be caused by viruses, parasites, bacterial neurotoxins, or unspecified trigeminal ganglion inflammation; seven cases with degenerative lesions caused by trauma, bacterial neurotoxins, and possibly unknown infectious agents; and four non-altered cases used as controls (**Supplementary Material 1**). Complete histological assessment and etiologic diagnosis of each case are also available at Boos (21). Samples were retrieved from the tissue archives of Brazilian Universities related to this study's authors and from the Institute of Veterinary Pathology in Giessen (non-altered controls). Samples consisted of formalin-fixed paraffin-embedded (FFPE) material archived at room temperature and protected from light. Standardized material was unavailable for all cases due to sampling of CNS regions of interest

during the necropsy of cases of natural disease and material availability after long-term storage. Therefore, CNS sections were categorized into four regions, according to Kaufmann et al. (22): (1) forebrain, (2) midbrain, (3) cerebellum, and (4) spinal cord.

Immunohistochemistry

From each CNS region available, sections with 4- μ m thickness were obtained and placed on glass slides SuperFrost® Plus Objektträger (R. Langenbrinck, Emmendingen, Germany). Slides were deparaffinized in xylol, followed by immersion in decreasing concentrations of ethanol. Endogenous peroxidase was blocked with 3% H₂O₂ in methanol for 20 min. To demonstrate GFAP, blocking of unspecific endogenous activity was carried out with 20% swine serum (B15-030, PAA Laboratories GmbH, Pasching, Austria) diluted in tris-buffered saline (TBS) for 10 min at room temperature. While for demonstration of Iba1, blocking was carried out with 1.5% goat serum (B11-035, PAA Laboratories GmbH, Pasching, Austria) diluted in 1% bovine serum albumin (BSA)/TBS for 1 h at room temperature. Negative controls consisting of the same CNS regions from every horse were incubated with rabbit-control serum (Dako A/S, Glostrup, Denmark) instead of primary antibody. Dilution and incubation of primary antibodies, secondary antibodies, and detection systems are described in **Table 1**.

Immunohistochemistry Quantitative Analysis

In each of the CNS regions immunostained with GFAP and with Iba1, the number of stained cells was counted in five lesioned and five non-lesioned microscopic fields magnified $\times 200$. This would ensure that cases containing only small tissue sections would be also analyzed, while cases containing larger sections would be sufficiently represented. Microscopic fields were selected according to the histological assessment performed by Boos (21) that defined where the lesioned and non-lesioned areas were. Microscopic images were captured by a Nikon Eclipse 80i microscope (Nikon, Düsseldorf, Germany) equipped with a digital camera Nikon DS-Fi1 and analyzed with the NIS-Elements Basic Research 3.2 64bit software (Nikon, Düsseldorf, Germany).

Immunohistochemistry Morphologic Analysis

The morphological criteria were determined by a board-certified veterinary pathologist (CH) and a Ph.D. student (GSB). Lesioned areas were further classified in sections that predominantly displayed inflammation or degenerative lesions. Furthermore, astrocytic (5, 8) and microglial (11, 23, 24) morphologic alterations were classified from non-altered (grade 0) to severely altered (grade 3), according to **Tables 2, 3**. Mid-scale values were also possible. The intensity of immunostaining was not considered for the scoring system, but annotations were made when meaningful. Furthermore, as Iba1 stains, not only resident microglia but also monocytes/macrophages that migrate from the periphery, the stained cells observed within blood vessels

TABLE 1 | Immunohistochemistry for astrocytes and microglia assessment in the CNS of horses.

Antibody	Source	Dilution	Secondary antibody	Detection system
GFAP, polyclonal rabbit	Z0334 Dako A/S, Glostrup, Denmark	1:500 in 20% swine serum, overnight, 4°C	Swine anti-rabbit ^a , 1:100 in 20% swine serum/TBS, 30 min, RT	PAP ^b , 1:600 in 1% BSA/TBS, 30 min, RT
Iba1, polyclonal rabbit	019-19741 Wako Chemicals GmbH, Neuss, Germany	1:500 in 1% goat/serum/1% BSA/TBS, overnight, 4°C	Biot. goat anti-rabbit ^c , 1:200 in 1.5% goat serum/1% BSA/TBS, 30 min, RT	ABC ^d , 9 µl (A+B)/ml of 1.5% goat serum/1% BSA/TBS, 30 min, RT

ABC, avidin–biotin complex; BSA, bovine serum albumin; GFAP, glial fibrillary acid protein; Iba1, ionized calcium-binding adapter molecule 1; PAP, peroxidase anti-peroxidase; RT, room temperature; TBS, tris-buffered saline.

^aSwine anti-rabbit IgG, Z0196, Dako A/S, Glostrup, Denmark.

^bMouse peroxidase-anti-peroxidase (PAP) antibody, 223-005-024, Jackson ImmunoResearch Laboratories Inc., West Grove, PA, USA.

^cBiotinylated goat anti-rabbit IgG, BA 1000, Vector Laboratories Inc., Burlingame, CA, USA.

^dVectastin[®] ABC Kit peroxidase standard, PK-4000, Vector Laboratories Inc., Burlingame, CA, USA.

TABLE 2 | Morphologic criteria to grade astrocytic injury in the CNS of horses according to GFAP staining.

Morphologic parameter	Severity of astrocytic alterations			
	Non-altered	Mild	Moderate	Severe
Apparent cellular proliferation	No	No or discrete	Moderate	Yes
Nucleus	No alterations	Mild increase in volume	Moderate increase in volume	Severe increase in volume, binucleated cells (gemistocytes)
Cytoplasm	Few mildly stained cells	Mildly stained	Moderately stained	Accentuated stain
Processes ^a	Long, thin, well-ramified	Long, thin, well-ramified	Long, moderately thickened	Thickened, trespassing other cells processes, glial scar formation
Grade	0	1	2	3

CNS, central nervous system; GFAP, glial fibrillary acidic protein.

^aProtoplasmic (in the gray matter, with numerous, shorter, and branched processes) and fibrous (in the white matter, with relatively few, long processes) astrocytes taken into consideration according to Sofroniew and Vinters (5).

TABLE 3 | Morphologic criteria to grade microglial proliferation/invasion in the CNS of horses according to Iba1 staining.

Morphologic parameter	Severity of microgliosis			
	Non-altered	Mild	Moderate	Severe
Apparent cellular proliferation	No	No or discrete	Moderate	Yes
Nucleus	No alterations	Mild increase in volume	Moderate increase in volume	Severe increase in volume
Cytoplasm	Few mildly stained cells	Mildly stained	Moderately stained	Accentuated stain or vacuolated (Gitter cell)
Processes	Long, thin, well-ramified	Long, thin, well-ramified	Long, moderately thickened (bushy cells)	Thickened and/or shortened, amoeboid shape, bipolar (rod cells)
Grade	0	1	2	3

CNS, central nervous system; Iba1, ionized calcium-binding adapter molecule 1.

were discarded from the scoring system. On the other hand, the pathological relevance of those cells was considered for discussion.

Statistical Analysis

Statistical tests were conducted with the statistical program packages BMDP/Dynamic Release 8.1 (Statistical Solutions Ltd.,

Cork, Ireland) (25) and StatXact 9.0 (26). According to the IHC quantitative and morphologic analysis, data were sorted with each of the four CNS regions available. Mean values, standard deviation, minima, maxima, and sample sizes were calculated and tabulated from quantitative analysis. In the semiquantitative variables, the data description was carried out by specifying the medians, the quartiles (Q1 and Q3), and the smallest and largest observations with the presentation in box and whisker plot. Graphical illustrations were generated with MS Excel.

Statistical Analysis of the Number of Glial Fibrillary Acidic Protein+ and Ionized Calcium-Binding Adapter Molecule 1+ Cells in Different Lesion Setups

Since the data included two repeated measurements per horse (lesioned and non-lesioned area), a *t*-test for dependent samples was conducted to determine if the mean number of GFAP+ and Iba1+ cells occurred differently between lesioned and non-lesioned areas of each CNS region. In the next analysis step, only the lesioned areas were kept in the data set. To determine if the mean number of GFAP+ and Iba1+ cells was significantly different with a different morphologic alteration grade (inflammatory infiltration and degenerative lesions), the Wilcoxon–Mann–Whitney test (WMWT) and the WMWT with exact inference were applied. Statistical significance was assigned as $p \leq 0.05$.

Statistical Analysis of Astrocytic and Microglial Grades of Alteration in Different Lesion Setups

Due to the ordinal scale as well as the high number of tied ranks in the data and the fact that data included two repeated measurements per horse (lesioned and non-lesioned area), the exact Wilcoxon signed-rank test was carried out. It was used to determine if there are differences in the astrocytic/microglial grade of lesioned and non-lesioned areas. To characterize the association between the range of astrocytes/microglial cells stained and the ordinality scaled astrogliosis/microgliosis grade, Spearman's rank correlation coefficient was computed. Also, statistical significance was assigned as $p \leq 0.05$.

RESULTS

Glial Fibrillary Acidic Protein Immunohistochemistry Morphologic Analysis

Morphologic alterations in astrocytes were compared with the immunostaining observed in the respective brain areas from four horses' non-altered CNS. Normal astrocytes from these controls were characterized by a light brown cytoplasmic GFAP staining, surrounded by long and thin processes, while the nucleus remained unstained (Figure 1, grade 0). Mild astrocytic alterations were characterized by cells with a mildly enlarged nucleus, with cytoplasm and processes still mildly stained (Figure 1, grade 1). As opposed to that, in brain regions presenting moderate (Figure 1, grade 2) and severe (Figure 1, grade 3) astrocytic alterations, there were marked morphologic alterations, such as nuclear enlargement and thickening of processes, allied to stronger immunostaining and gemistocytes

observed in grade 3 (horses 4 and 29). In some cases of grade 3, the cellular nucleus appeared vacuolated (Figure 1, midbrain). However, in the spinal cord, none of the samples studied displayed morphological alterations compatible with grade 3. The range of GFAP+ cells found in each grade of alteration is demonstrated in Figure 1.

Regarding a possible pathological relation, for cases with inflammation (28/35), 14/28 had a viral infection, which displayed mostly mild-to-moderate astrocytic alterations (10/14), followed by severe alterations in 4/14. There were moderate alterations in protoplasmic and fibrous astrocytes of all cases of parasitic infections, while cases of local ganglion inflammation had mild astrocytic alterations in the CNS. Cases suggestive of bacterial neurotoxin lesions were represented by inflammatory and degenerative lesions, presenting all alteration grades. Traumatic degenerative lesions and unknown infectious pathogens causing degeneration presented moderate alterations (Figure 1).

Determination of the Number of Glial Fibrillary Acidic Protein+ Cells in Different Lesion Setups

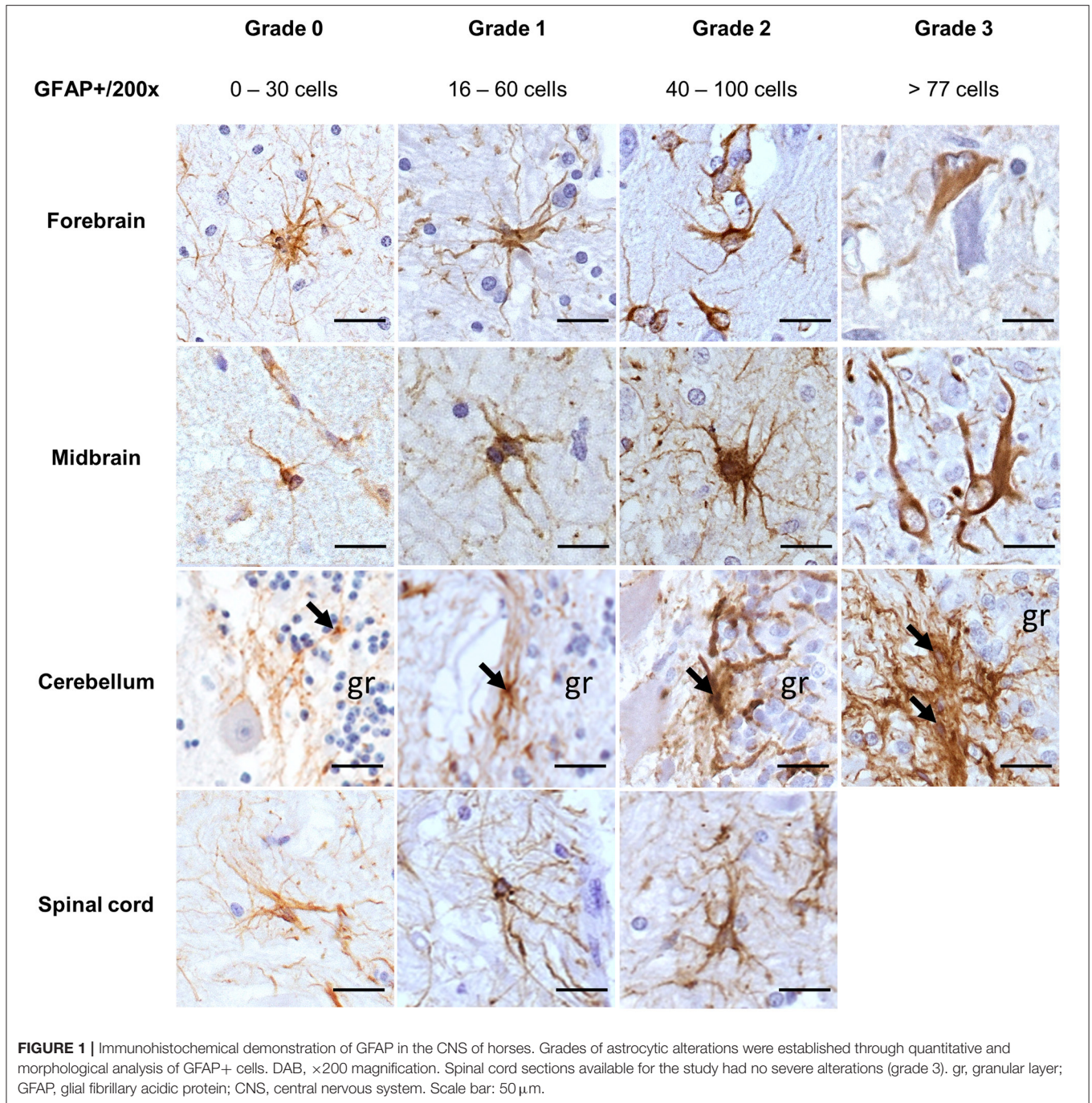
The *t*-test for dependent samples showed a statistically significantly higher number of GFAP+ cells in lesioned areas than in non-lesioned areas from all four CNS regions of all 35 horses investigated, namely, the forebrain [$t_{(24)} = 6.3, p < 0.001$], midbrain [$t_{(13)} = 4.22, p = 0.001$], cerebellum [$t_{(11)} = 5.26, p < 0.001$], and spinal cord [$t_{(21)} = 11.01, p < 0.001$] (Figure 2A). The median number of GFAP+ cells among the 35 horses was also higher in inflammatory lesions (median = 70.4) than in degenerative lesions (median = 37.8) in the midbrain ($U = 38.5, p < 0.05$), demonstrated with the WMWT (Figure 2B).

Comparison of Astrocytic Grades of Alteration in Different Lesion Setups

The Wilcoxon signed-rank test indicated that lesioned areas presented statistically significantly higher grades of morphologic alteration than non-lesioned areas in all CNS regions ($p < 0.001$) in general in all 35 cases (Figure 3A). The WMWT with exact inference demonstrated that the grade of astrogliosis was not statistically significantly different between inflammatory and degenerative lesions ($p \geq 0.05$) (Figure 3B). Spearman's rank correlation coefficient revealed that there was, in general, a positive correlation between the increase in the mean of GFAP+ cells and the increase in grade of astrocytic activation in lesioned brain areas (Figure 3C). Stronger correlations were observed in the forebrain and midbrain regions. Mid-scale grades like 1.5 and 2.5 were also observed and could indicate the continuous morphological changes in the tissue, with different stages of alteration in the same area.

Ionized Calcium-Binding Adapter Molecule 1 Immunohistochemistry Morphologic Analysis

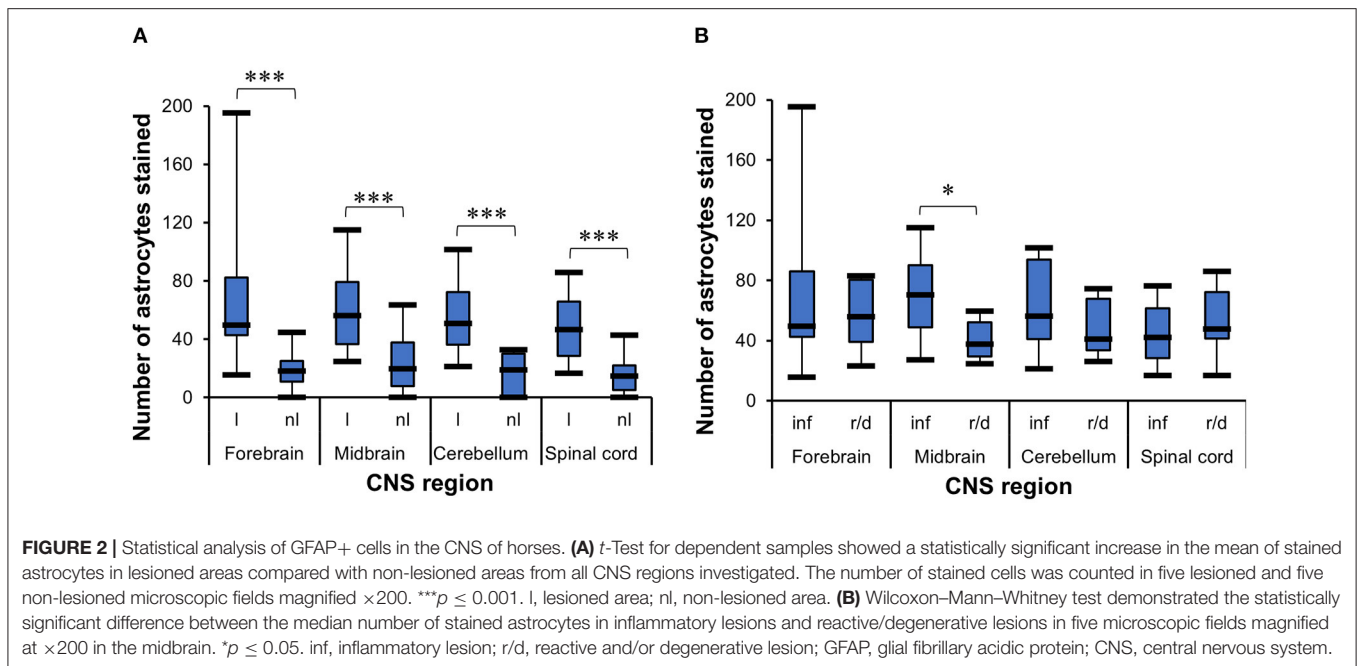
Iba1 demonstrated resting microglia in the CNS in the four non-altered controls and 6/35 cases (Figure 4, grade 0). Microglia cells were scattered and light-stained, with ramified cytoplasm and oval to elongated or bean-shaped nuclei. Mild microglial



alterations were associated with a slight thickening of cellular processes and nucleus rounding. In these cases, a mildly darker cytoplasm was also observed (Figure 4, grade 1). For moderate alterations, microglia cells had “bushy” features, but most of the cells still presented ramifications (Figure 4, grade 2). On the other hand, severely altered Iba1+ cells had retracted ramifications, and the cells had an amoeboid shape and were deeply stained (Figure 4, grade 3). Morphology compatible with Gitter cells was demonstrated by cells with bulky cytoplasm

strongly stained on the borders, decreasing in intensity when reaching the cell center, while the nucleus, when visible, was unstained (Figure 4, grade 3, forebrain). In general, in grade 3 of alteration, it was impossible to differentiate microglia from macrophages recruited from the periphery when they were amidst the tissue; in some cases, groups of densely packed Iba1+ cells were seen within vessels, also in grade 3 tissues.

Regarding the pathology associated with the cases studied, most of the viral infections presented at least one region of the



CNS with mild microglial activation (12/14 cases). This mild activation was accompanied by resting microglia (6/12) or by grade 2 microglia (2/12). There was one case with moderate microglial activation (horse 29) and another one with severe alterations (horse 27) (**Supplementary Material 1**). For parasitic infections, there were two distinctive stages: in 3/6 cases that were characterized with mild inflammatory lesions, there was also mild microgliosis, while in the other 3/6 cases with severe inflammatory lesions, microgliosis ranged from moderate to severe. Cases of local ganglion inflammation presented only resting microglia in the CNS. Similarly, 3/6 cases suggested to have suffered from bacterial neurotoxins showed non-altered microglia, while the other 3/6 had grade 1 alterations. Traumatic degenerative lesions and unknown infectious pathogens causing degeneration presented moderate-to-severe and mild microglial activation, respectively.

Additionally, microglial nodules were present in 7/35 cases—five with a viral infection and two with parasitic infection (protozoa)—formed by large and compact groups of strongly stained cells (**Figure 5A**). Iba1+ cells were also demonstrated accompanying satellite cells around neurons and/or during neuronophagia in 18/35 cases (**Figures 5B,C**). These features were observed in 11/14 cases of viral infection, 1/4 case of an unknown pathogen, 5/6 cases of parasitic infection, and 1/6 cases of suggested bacterial toxic infection.

Determination of the Number of Ionized Calcium-Binding Adapter Molecule 1+ Cells in Different Lesion Setups

The *t*-test for dependent samples showed that there was a statistically significantly higher mean of Iba1+ cells in the lesioned areas from forebrain [$t_{(24)} = 3.87, p = 0.007$], midbrain [$t_{(13)} = 3.31, p = 0.0056$], and spinal cord [$t_{(21)} = 3.02, p =$

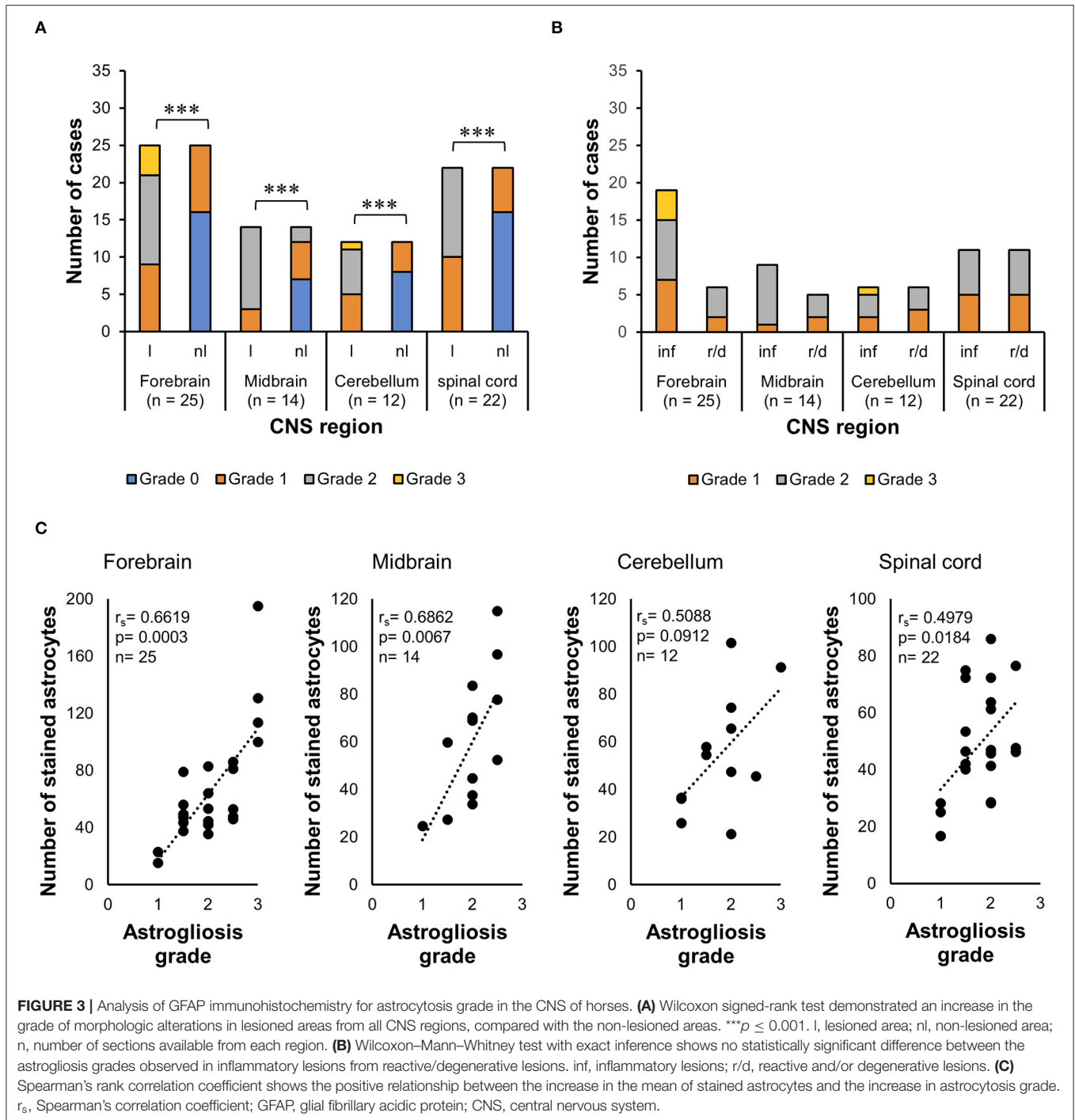
0.0065] than in non-lesioned areas, but there was no statistical difference in cerebellum [$t_{(11)} = 1.25, p = 0.2365$] (**Figure 6A**). The WMWT indicated that the median of Iba1+ cells was higher in inflammatory lesions (median = 32) than in degenerative lesions (median = 9.4) only in the midbrain ($U = 39.5, p = 0.0230$) (**Figure 6B**). From the pathogenetic view, this could indicate a shift toward lesions caused by viruses and parasites and a possible tropism for this brain area.

Comparison of Microglial Grades of Alteration in Different Lesion Setups

The Wilcoxon signed-rank test indicated that lesioned areas also presented statistically significant higher morphologic alteration grades than non-lesioned areas ($p < 0.001$) in the midbrain ($p = 0.0020$) and spinal cord ($p < 0.001$), but not in the cerebellum ($p = 0.5313$) (**Figure 7A**). The WMWT with exact inference demonstrated that the microgliosis grade of inflammatory lesions in the midbrain was statistically significantly higher than that of degenerative lesions ($p = 0.0070$) (**Figure 7B**). In the spinal cord sections, the inflammatory lesions also showed higher activation grades, but this difference did not reach statistical significance. Spearman's rank correlation coefficient revealed that there was generally a positive relationship between the increase in the mean of Iba1+ cells and the increase in the grade of microglial activation in the lesioned areas of the CNS (**Figure 7C**). Mid-scale grades like 1.5 and 2.5 were also observed and could indicate continuous morphological changes in the tissue, with different stages of alteration in the same area.

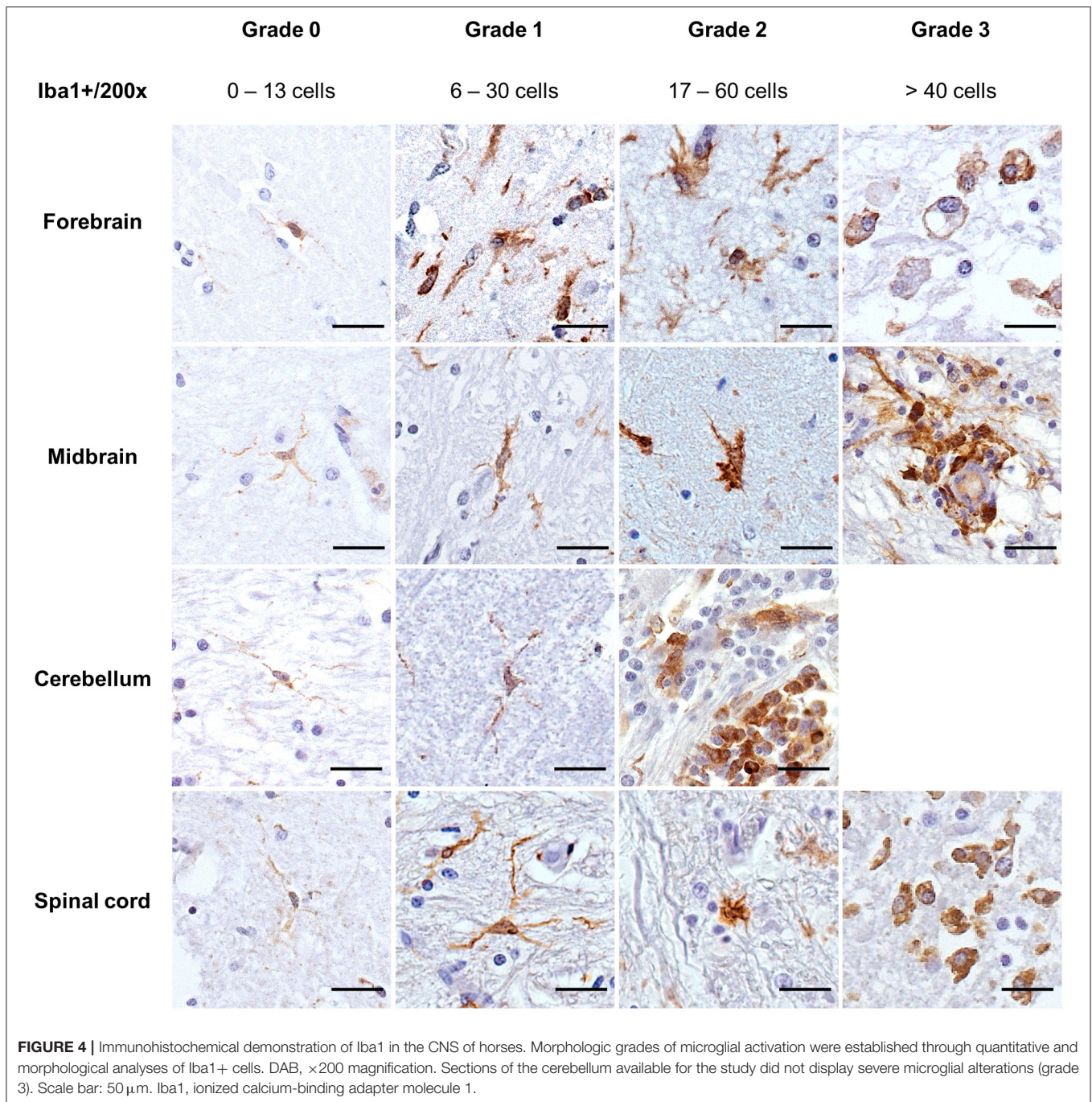
DISCUSSION

Like humans, horses are susceptible to neurotropic and neuroinvasive pathogens that are not always readily identified



in histological sections. Instead, alterations in astrocytes and microglia cells can be used as pathological hallmarks of injured nervous tissue in a variety of infectious and degenerative diseases (7). However, equine glial cell alterations are yet poorly characterized. Studies that demonstrate astrocytic and microglial activation in the CNS of horses have so far focused on describing morphological alterations associated with a known disease/alteration (2, 4).

Therefore, in this study, quantitative and morphological profiles of astrocytes and microglia of horses were translated into a scoring system, which was statistically verified using 35 cases of encephalitis/encephalopathies and four non-altered controls. This scoring system could also help to identify alterations undergone by glial cells when an etiology is undetermined, using the vastly used IHC markers GFAP and Iba1. Furthermore, recent studies with machine learning methods could benefit from this

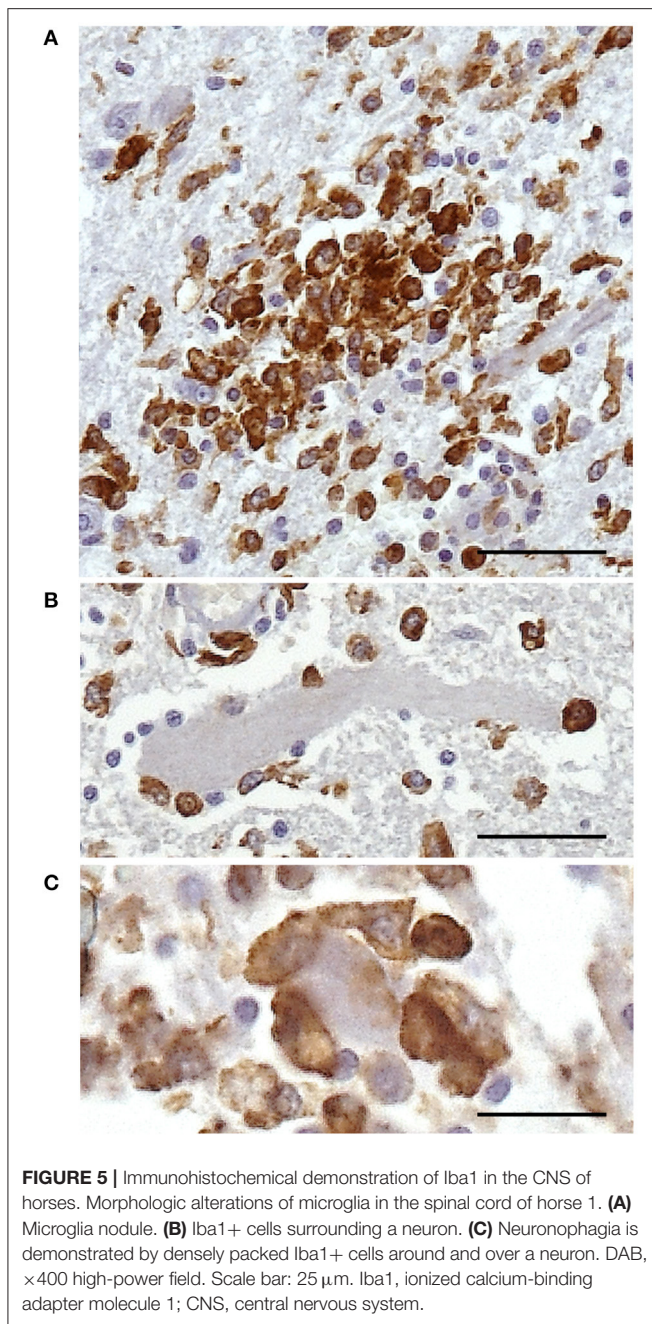


score, as it would provide a morphological template of different stages of alteration to complement quantification algorithms (12, 13).

Immunohistochemical Demonstration of Equine Astrocytes

In this study, normal astrocytes (grade 0) appeared as staining in a range of 0 to 30 astrocytes/×200 magnification that were well-ramified with minimal contact between cells and tightly connected with blood vessels as also described in the spinal cord

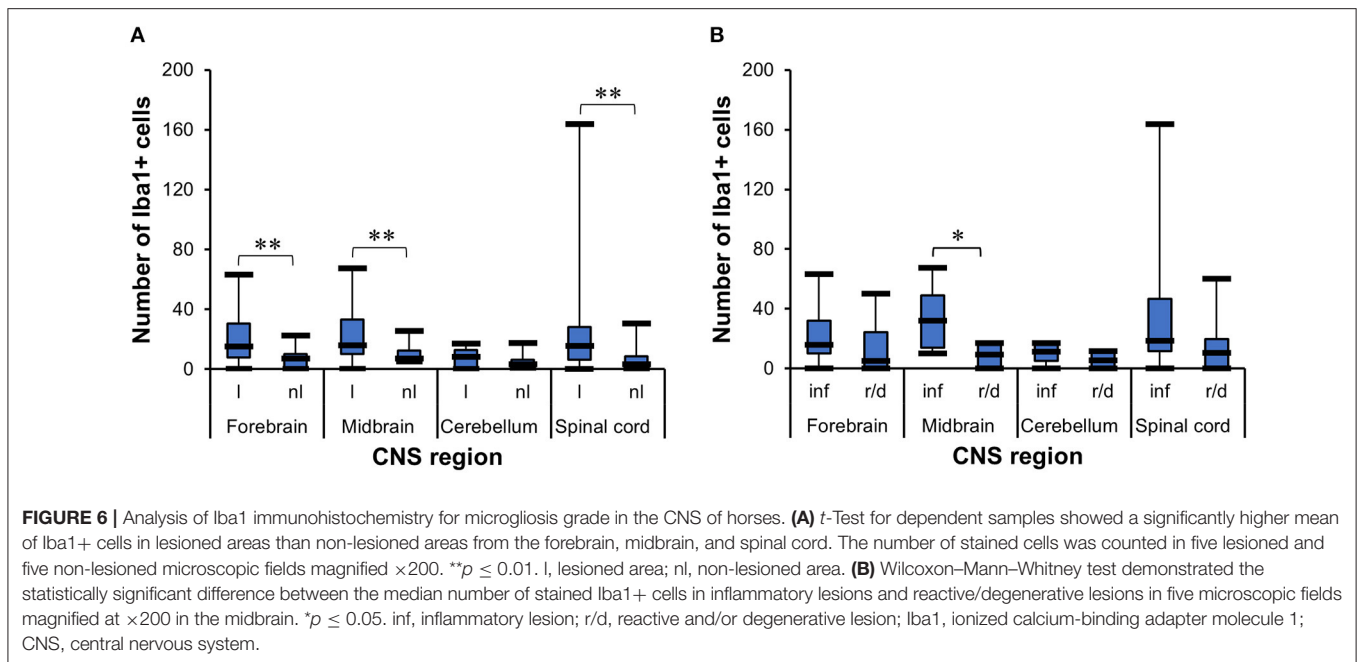
of horses by Meneses et al. (27) and in fibrous astrocytes from the cerebral cortex in control horses from Regina et al. (28). Studies in other animal species describe a similar morphology in non-altered CNS of dogs (29), mice (30), and rats (31), but cattle have a higher number of GFAP+ cells and non-altered astrocytes approximate morphologically to our grade 1 for horses (32). Limited or no proliferation of astrocytes was observed in mouse models of Alzheimer's disease and amyotrophic lateral sclerosis (33–35). In mild astrogliosis (grade 1), slight astrocytic morphologic alterations consisted of mild



nuclear enlargement and an apparent increase in positive cells, ranging from 16 to 60/×200 magnification. These features were also described by Campos et al. (36) and de Sousa et al. (37) in the astrocytes from horses infected with the arbovirus Eastern equine encephalitis virus (EEEV) and match with the findings in this study in horses 24–27 and 32. There were mild alterations also in the rabies virus case (horse 2), with a comparable number and morphology of astrocytes found at the beginning of the infection demonstrated in the spinal cord of mice (38). Although there are no reports on grading from equine astrocytes in the literature, some authors described at

least the increase in the number of GFAP+ cells in lesioned brain areas compared with normal horse brains (2, 4) or in studies about canine visceral leishmaniasis (39), canine distemper disease (40), and rhesus macaques with neurobrucellosis (41). Mild astrocytic activation was also observed in at least one non-altered region of the CNS of cases with degenerative lesions (like in horses 12, 14, 16, 17, and 28), associated with more severe alterations in other brain areas. This feature was already reported in neurotoxic events induced by mycotic, plant, and botulinum toxins, and uremic/hepatic encephalopathy (42–46). In moderate astrogliosis (grade 2), there were 40 to 100 GFAP+ cells/×200 magnification, accompanied by a more prominent cellular hypertrophy, and astrocytic processes overlapped. With this configuration, suggested parasitic infections like those displayed by horses 1, 9, 18, 19, 20, and 22 are supported by the findings demonstrated in mice experimentally infected with *Toxocara canis* (47, 48) and pigs with neurocysticercosis (49). On the other hand, Lemos and Alessi (28) found that astrocytes from horses suffering from leucoencephalomalacia displayed morphological alterations compatible with our grade 2, but with fewer GFAP+ cells. These findings justify the importance to address morphological and quantitative alterations of astrocytes in different pathological settings. Severe astrogliosis (grade 3) was associated with pronounced GFAP immunostaining and more than 77 GFAP+ astrocytes/×200 magnification with severe alterations. Like in severe human astrogliosis, there was pronounced cellular hypertrophy of the cell body and processes in horses. There was substantial intermingling and overlapping of neighboring astrocyte processes with blurring and disruption of individual astrocyte domains, as described by Sofroniew and Vinters (5). In the literature, this severe diffuse reaction pattern is described in severe focal lesions, infections, and chronic neurodegeneration (5). Comparably, all horses with grade 3 astrogliosis also had some degree of inflammatory lesions that were caused by a virus (horses 4, 24, 27, and 33) or a toxin (horse 11). Occasionally, gemistocytes were seen in the forebrain of horse 4 and midbrain of horse 29, which occur when there is lethal injury toward astrocytes, and in these cases, they were associated with arbovirus infections (16, 40). Upon a flaviviral infection, highly activated astrocytes increase their production of GFAP, which, combined with the release of inflammatory cytokines and chemokines by other components of the CNS, can lead to a severe course of the disease with a higher fatality rate (50, 51). Moreover, differences in protoplasmic and fibrous astrocytes were not explored at length since most of the lesions were observed in the gray matter. When present, lesions in the white matter were associated with cases of protozoan infections in the spinal cord (grade 2) and degenerative myelopathies (grade 2), similar to the cases of equine back pain from Mayaki et al. (52).

The statistical analysis carried out with the equine samples supported the morphological astrocytic alterations translated into the scoring system established. Correlation tests indicated that lesioned areas have a higher number ($p \leq 0.05$) of GFAP+ astrocytes than non-lesioned areas and higher astrocytic alteration grades, independently of an inflammatory or degenerative lesion that triggered the response. The positive correlation obtained with a Spearman's rank correlation



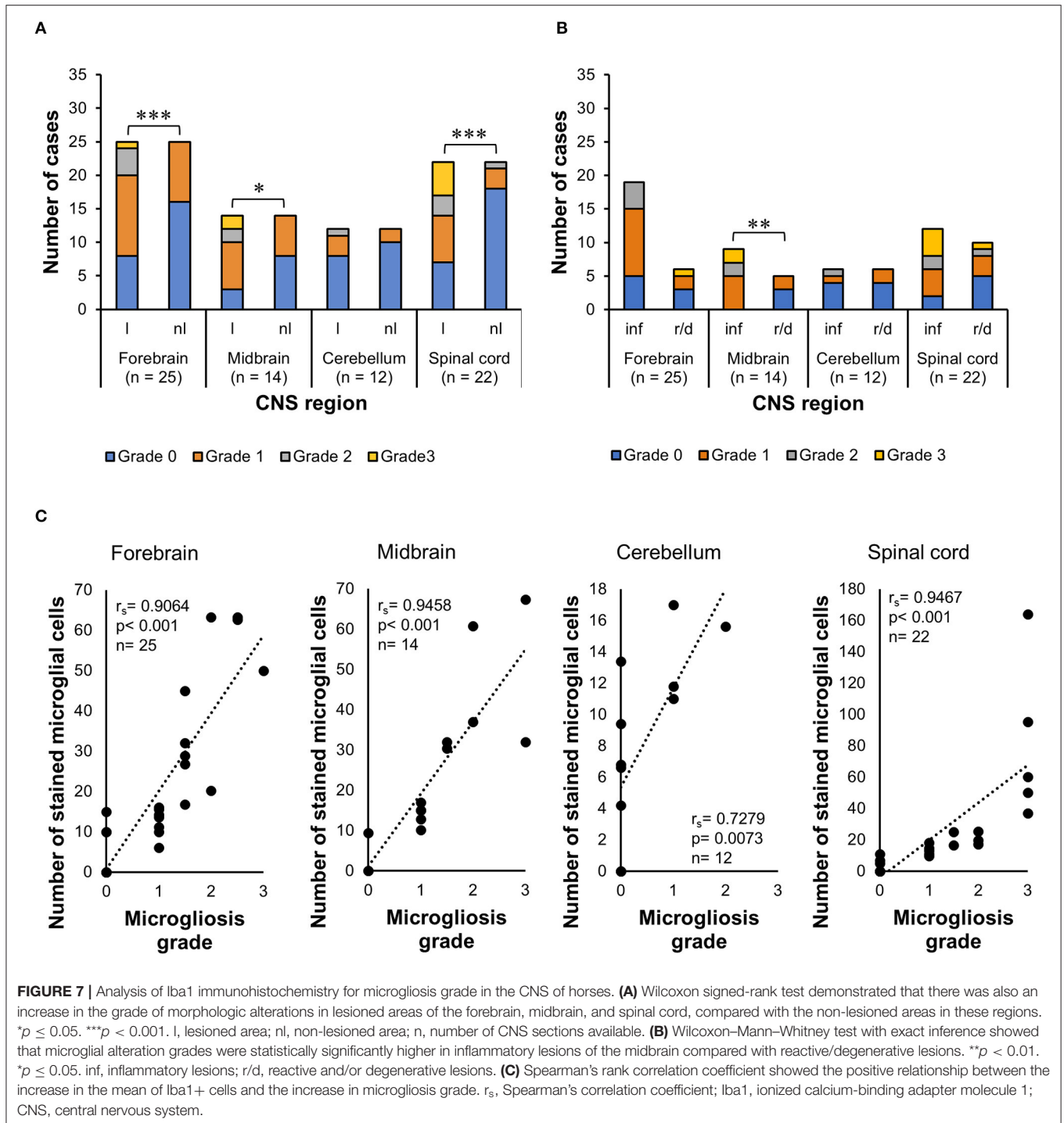
coefficient showed that the astrogliosis grades were correctly designated, as the higher the number of GFAP+ cells, the more severe were the morphological alterations.

The statistical model established for equine samples addressed some of the missing aspects regarding astrocytic reactions in horses. As observed in humans, astrogliosis in horses occurs in a spectrum of heterogeneous changes, translated into alteration grades (grades 1, 2, and 3) in this study. Besides, astrogliosis is widely used as a hallmark of diseased CNS tissue, thus the correct designation of morphologic and quantitative astrocytic alterations, which were missing for horses, can also help to relate certain pathogens/conditions in unresolved cases of encephalitis and encephalopathies.

Immunohistochemical Demonstration of Equine Microglia Cells

Resting microglia (grade 0) were characterized by faintly stained cells that exhibited ramified and slender processes, with inconspicuous, small, hyperchromatic, and wedge-shaped nucleus, also observed by other authors (1). Resting microglia were found in all four non-altered equine brains used as controls, in non-lesioned areas bordering lesions, and in CNS regions completely lesion-free (but in cases with alterations in other sections). A similar morphology of resting microglia was described in early studies of microglia features (23), in mice (30), and the equine non-altered controls from an experimental study with *Trypanosoma evansi* infection (2). A mild microglial activation (grade 1) was characterized by a range of 6 to 30 Iba1+ cells/ $\times 200$ magnification, and the morphological alterations were discrete, inclined to the beginning of cellular processes retraction. Grade 1 was the highest alteration observed in 17/35 cases, and although there are no reports of solely mild microgliosis as the main microglial alteration in horses, resting microglia are progressively activated in traumatic injuries, ischemic stroke,

demyelination, and neurodegenerative diseases (53). In the four cases described as flaviviral infection (horses 3 to 6), this pattern was also observed and could indicate a delay in the immunological answer of microglia cells toward these pathogens (54). Flaviviruses, among other viruses, might invade the CNS through Trojan horse mechanisms, remain undetected by the host immune system for a longer period, and cause further neurological alterations (54). In other 4/35 cases (horses 10, 24, 26, and 27), this mild activation was associated with more severe grades in other CNS regions. In the moderate level of activation (grade 2) observed in 5/35 cases (horses 15, 23, 24, 26, and 29), a range of 17 to 60 cells/ $\times 200$ magnification were demonstrated with distinguishable cellular processes retraction, and a general hypertrophic reaction with an increased number of Iba1+ cells, also described by other studies (16, 53, 55). Grade 3 microglia activation was observed in 7/35 cases and was associated with Gitter cell occurrence. These bulky cells, peripherally stained with Iba1, were observed concurrently with other smaller, densely packed, and intensely stained microglia. These activated smaller cells were also seen within vessels, a sign of peripheral migration of monocytes as reported in severe microgliosis associated with blood–brain barrier damage in experimental autoimmune encephalomyelitis (14). Furthermore, Gitter cells were observed within brain areas of horses displaying inflammatory lesions caused by parasites (horses 1, 9, and 22), viruses (horses 7 and 27), and toxins (horse 10) and in a case with degenerative spinal cord of unknown origin (horse 8). Other studies that assessed equine microglia demonstrated these highly activated cells in lesions produced in equine protozoan myeloencephalitis (2, 56, 57), by *Halicephalobus gingivalis* (58), rabies virus (59), *Trema micrantha* intoxication (60), and leucoencephalomalacia by mycotoxicosis (44). Furthermore, moderate-to-severe microgliosis was statistically associated with inflammation in the midbrain, with a tendency to occur in



viral (horses 24, 27, and 29) and parasitic infections (horse 22). This feature could indicate a tropism from the pathogen to this brain area.

The statistical analysis also supported the morphological aspects attributed to the scoring system. Correlation tests indicated that lesioned areas from the forebrain, midbrain, and spinal cord have a higher number ($p \leq 0.05$) of Iba1+ cells than non-lesioned areas, as well as higher microglial activation

grade. Cerebellum sections were underrepresented in the study, which could have influenced the statistical analysis's lack of correlation. The positive correlation obtained with a Spearman's rank correlation coefficient showed that the microglia activation grades were correctly designated, as the higher the number of Iba1+ cells, the more severe were the morphological alterations.

Other interesting features of microglial activation in the CNS of horses and that could help assess an etiology underlying

the alterations observed are microglial nodules; observed in 7/35 cases that presented non-suppurative encephalitis. It is still debatable if different pathogens (viruses vs. parasites) induce different glial reaction patterns. However, we confirmed in our study the predominance of microglial nodule formation by viral infections in horses (in 5/7 cases) (4, 59, 61, 62). For the other two cases (horses 1 and 9), a protozoal infection was detected, and the nodule formation could indicate the persistence of neurophagic sites (63). Furthermore, neuronophagia was commonly observed among the cases studied (18/35), with no predominance for an activation grade. However, there was a strong tendency to occur in samples with inflammation, as a feature of many viral infections (16). Additionally, reactive microglia also develop into rod cells, a bipolar ramified configuration. Again, these are most commonly seen in neurotropic viral diseases, like Borna disease in horses (16), but are also reported in human cases of subacute sclerosing panencephalitis, Alzheimer's disease, and Wilson's disease (64) and in horses experimentally infected with *T. evansi* (2). Although their function is not entirely understood, they are observed when there is diffuse brain injury (11, 65), going along with the extensive and severe lesions observed in tissues from horses 1 and 22 in this study.

CONCLUSIONS

The statistical model established in this study addressed some of the missing aspects regarding astrocytic and microglial reactions in horses. Like observed in humans, these alterations occur in a spectrum of heterogeneous changes, here translated into grades 1, 2, and 3. Also, astrogliosis and microgliosis are widely used as a hallmark of diseased CNS tissue, and therefore, the correct designation of morphologic and quantitative alterations, which were missing for horses, can also help to relate certain etiologies in unresolved cases of encephalitis and encephalopathies. Moreover, this study can serve as a template for studies in segments of artificial intelligence to quantify glial cells. On the other hand, the lack of complete CNS sets in all cases can be a limitation if a profound assessment of the alterations undergone by each etiology is sought. However, on a routine basis in diagnostics, pathologists hardly have all CNS areas available, and the center of interest for investigation is sections with lesions, which were well-represented in the study.

DATA AVAILABILITY STATEMENT

The raw data supporting the conclusions of this article will be made available by the authors, without undue reservation.

REFERENCES

1. Delcambre GH, Liu J, Herrington JM, Vallario K, Long MT. Immunohistochemistry for the detection of neural and inflammatory cells in equine brain tissue. *PeerJ*. (2016) 4:e1601. doi: 10.7717/peerj.1601
2. Lemos KR, Marques LC, Aquino LPCT, Alessi AC, Zacarias RZ. Astrocytic and microglial response and histopathological changes in the brain of horses

ETHICS STATEMENT

Ethical review and approval was not required for the animal study because this work was carried out with archived material formalin-fixed paraffin-embedded. Written informed consent for participation was not obtained from the owners because this work was carried out with archived material formalin-fixed paraffin-embedded. There is no mention on names, specific places, or any other form that would allow the identification of owners and animals.

AUTHOR CONTRIBUTIONS

GB contributed to the conception, designed the study, and organized and wrote the manuscript. KF performed the statistical analysis. EC, DD, MC, DB, and JD collected the samples and provided clinical and histological reports. CH contributed to the conception, design of the study, and manuscript writing. All authors revised the manuscript revision and read and approved the submitted version.

FUNDING

This study was supported by the Brazilian Coordination of Superior Level Staff Improvement (CAPES), National Council for Scientific and Technological Development (CNPq), and the German Academic Exchange Service (DAAD), under the process number 490235/2013-1. The Open Access to this study was funded by the Justus-Liebig-University, Giessen.

ACKNOWLEDGMENTS

Parts of this manuscript were published in the Ph.D. thesis of GB. We would like to thank the Unit for Biomathematics and Data Processing from the Justus Liebig University Giessen (Kathrin Büttner and Marion Sparenberg) for statistical advice and Luciana Sonne, Fabiana Marques Boabaid, Adriana Gomes, and Susy Karoline Hermes de Sousa for the support in the gathering of material and information. We also thank Alexandra Luh for the excellent technical support.

SUPPLEMENTARY MATERIAL

The Supplementary Material for this article can be found online at: <https://www.frontiersin.org/articles/10.3389/fvets.2021.660022/full#supplementary-material>

with experimental chronic *Trypanosoma evansi* infection. *Rev Inst Med Trop São Paulo*. (2008) 50:243–9. doi: 10.1590/S0036-46652008000400011

3. Salouci M, Antoine N, Shikh Al Sook MK, Piret J, Mignon Y, Kirschvink N, et al. Developmental profiles of GFAP-positive astrocytes in sheep cerebellum. *Vet Res Commun*. (2014) 38:279–85. doi: 10.1007/s11259-014-9614-1
4. Delcambre GH, Liu J, Streit WJ, Shaw GPJ, Vallario K, Herrington J, et al. Phenotypic characterisation of cell populations in the brains of horses

- experimentally infected with West Nile virus. *Equine Vet J.* (2017) 49:815–20. doi: 10.1111/evj.12697
5. Sofroniew MV, Vinters HV. Astrocytes: biology and pathology. *Acta Neuropathol.* (2010) 119:7–35. doi: 10.1007/s00401-009-0619-8
 6. Pekny M, Pekna M. Astrocyte reactivity and reactive astrogliosis: costs and benefits. *Physiol Rev.* (2014) 94:1077–98. doi: 10.1152/physrev.00041.2013
 7. Kovacs GG. Cellular reactions of the central nervous system. In: Kovacs GG, Alafuzoff I, editors. *Handbook of Clinical Neurology.* 1st ed. Amsterdam: Elsevier B.V. (2018). p. 13–23.
 8. Sofroniew MV. Molecular dissection of reactive astrogliosis and glial scar. *Trends Neurosci.* (2009) 32:638–47. doi: 10.1016/j.tins.2009.08.002
 9. Shapiro LA, Perez ZD, Foresti ML, Arisi GM, Ribak CE. Morphological and ultrastructural features of Iba1-immunolabeled microglial cells in the hippocampal dentate gyrus. *Brain Res.* (2009) 1266:29–36. doi: 10.1016/j.brainres.2009.02.031
 10. Ziebell JM, Taylor SE, Cao T, Harrison JL, Lifshitz J. Rod microglia: elongation, alignment, and coupling to form trains across the somatosensory cortex after experimental diffuse brain injury. *J Neuroinflamm.* (2012) 9:247. doi: 10.1186/1742-2094-9-247
 11. Taylor SE, Morganti-Kossmann C, Lifshitz J, Ziebell JM. Rod microglia: a morphological definition. *PLoS ONE.* (2014) 9:e97096. doi: 10.1371/journal.pone.0097096
 12. Liu M, Ylanko J, Weekman E, Beckett T, Andrews D, McLaurin J. Utilizing supervised machine learning to identify microglia and astrocytes *in situ*: implications for large-scale image analysis and quantification. *J Neurosci Methods.* (2019) 328:108424. doi: 10.1016/j.jneumeth.2019.108424
 13. Healy S, McMahon J, FitzGerald U. Seeing the wood for the trees: towards improved quantification of glial cells in central nervous system tissue. *Neural Regen Res.* (2018) 13:1520. doi: 10.4103/1673-5374.235222
 14. Ajami B, Bennett JL, Krieger C, McNagny KM, Rossi FM V. Infiltrating monocytes trigger EAE progression, but do not contribute to the resident microglia pool. *Nat Neurosci.* (2011) 14:1142–9. doi: 10.1038/nn.2887
 15. Serrano-Pozo A, Gómez-Isla T, Growdon JH, Froesch MP, Hyman BT. A phenotypic change but not proliferation underlies glial responses in Alzheimer disease. *Am J Pathol.* (2013) 182:2332–44. doi: 10.1016/j.ajpath.2013.02.031
 16. Cantile C, Youssef S. Nervous system. In: Maxie G, editor. *Jubb, Kennedy & Palmer's Pathology of Domestic Animals. Sixth.* Saint Louis, MO: Elsevier (2016). p. 250–406.
 17. Angenvoort J, Brault AC, Bowen RA, Groschup MH. West Nile viral infection of equids. *Vet Microbiol.* (2013) 167:168–80. doi: 10.1016/j.vetmic.2013.08.013
 18. Bender JB, Tsukayama DT. Horses and the risk of zoonotic infections. *Vet Clin North Am - Equine Pract.* (2004) 20:643–53. doi: 10.1016/j.cveq.2004.07.003
 19. Kumar B, Manuja A, Gulati B, Virmani N, Tripathi BN. Zoonotic viral diseases of equines and their impact on human and animal health. *Open Virol J.* (2018) 12:80–98. doi: 10.2174/1874357901812010080
 20. Meneses CS, Müller HY, Herzberg DE, Uberti B, Werner MP, Bustamante HA. Microglia and astrocyte activation in the spinal cord of lame horses. *Vet Anaesth Analg.* (2018) 45:92–102. doi: 10.1016/j.vaa.2017.10.001
 21. Boos GS. *Non-suppurative Encephalitis and Encephalopathies of Unknown Origin in Horses From Brazil.* Justus-Liebig-University, Giessen (2020).
 22. Kaufmann W, Bolon B, Bradley A, Butt M, Czasch S, Garman RH, et al. Proliferative and nonproliferative lesions of the rat and mouse central and peripheral nervous systems. *Toxicol Pathol.* (2012) 40:87–157S. doi: 10.1177/0192623312439125
 23. Kreutzberg GW. Microglia: a sensor for pathological events in the CNS. *Trends Neurosci.* (1996) 19:312–8. doi: 10.1016/0166-2236(96)10049-7
 24. Lemstra AW, Groen in't Woud JCM, Hoozemans JJM, van Haastert ES, Rozemuller AJM, Eikelenboom P, et al. Microglia activation in sepsis: a case-control study. *J Neuroinflammation.* (2007) 4:4. doi: 10.1186/1742-2094-4-4
 25. Dixon WJ. *BMDP Statistical Software Manual 1992: BMDP Release 7 v.1.* Los Angeles, CA: University of California Press (1993). p. 698.
 26. CYTEL Inc. Cytel Studio StatXact Version 9.0.0. In: CYTEL Software Corporation, editor. *Statistical Software for Exact Nonparametric Inference, User Manual.* Cambridge, MA: CYTEL Inc. (2010).
 27. Meneses CS, Müller HY, Herzberg DE, Uberti B, Bustamante HA, Werner MP. Immunofluorescence characterization of spinal cord dorsal horn microglia and astrocytes in horses. *PeerJ.* (2017) 5:e3965. doi: 10.7717/peerj.3965
 28. Regina K, Carlos A, R ALK, Glial AAC, Veterinária P, Depto B, et al. Astrócitos imunorreativos à proteína glial fibrilar ácida (GFAP) em sistema nervoso central de equinos normais e de equinos com leucoencefalomalácia. *Pesqui Vet Bras.* (1999) 19:104–8. doi: 10.1590/S0100-736X1999000300003
 29. Hwang IK, Choi JH, Li H, Yoo K-Y, Kim DW, Lee CH, et al. Changes in glial fibrillary acidic protein immunoreactivity in the dentate gyrus and hippocampus proper of adult and aged dogs. *J Vet Med Sci.* (2008) 70:965–9. doi: 10.1292/jvms.70.965
 30. Kim JW, Nam SM, Yoo DY, Jung HY, Hwang IK, Seong JK, et al. Strain-specific differential expression of astrocytes and microglia in the mouse hippocampus. *Brain Behav.* (2018) 8:e00961. doi: 10.1002/brb3.961
 31. Kálmán M, Hajós F. Distribution of glial fibrillary acidic protein (GFAP)-immunoreactive astrocytes in the rat brain - I. Forebrain. *Exp Brain Res.* (1989) 78:147–63. doi: 10.1007/BF00230694
 32. Machado GF, Alessi AC. Astrócitos imunorreativos à proteína glial fibrilar ácida (GFAP) em SNC de bovinos normais e de bovinos com raiva. I. Hipocampo e giro dentado. *Brazilian J Vet Res Anim Sci.* (1997) 34:345. doi: 10.11606/issn.2318-3659.v34i6p345-348
 33. Kamphuis W, Orre M, Kooijman L, Dahmen M, Hol EM. Differential cell proliferation in the cortex of the APPswePS1dE9 Alzheimer's disease mouse model. *Glia.* (2012) 60:615–29. doi: 10.1002/glia.22295
 34. Sirko S, Behrendt G, Johansson PA, Tripathi P, Costa MR, Bek S, et al. Reactive glia in the injured brain acquire stem cell properties in response to sonic hedgehog. *Cell Stem Cell.* (2013) 12:426–39. doi: 10.1016/j.stem.2013.01.019
 35. Lepore AC, Dejea C, Carmen J, Rauck B, Kerr DA, Sofroniew MV, et al. Selective ablation of proliferating astrocytes does not affect disease outcome in either acute or chronic models of motor neuron degeneration. *Exp Neurol.* (2008) 211:423–32. doi: 10.1016/j.expneurol.2008.02.020
 36. Campos KF, Oliveira CHS De, Reis AB, Yamasaki EM, Brito MF, Andrade SJT, et al. Surto de encefalomielite equina Leste na Ilha de Marajó, Pará. *Pesqui Vet Bras.* (2013) 33:443–8. doi: 10.1590/S0100-736X2013000400005
 37. De Sousa SKH, Sonne L, Sant'Ana FJF de, Junior JLR. Encefalomielite equina do leste no Distrito Federal e entorno. *Acta Sci Vet.* (2015) 43:1–6. Available online at: <http://www.ufrgs.br/actavet/43/PUB%201268.pdf>
 38. Kojima D, Park C-H, Satoh Y, Inoue S, Noguchi A, Oyamad T. Pathology of the spinal cord of C57BL/6J mice infected with rabies virus (CVS-11 strain). *J Vet Med Sci.* (2009) 71:319–24. doi: 10.1292/jvms.71.319
 39. Melo GD, Machado GF. Glial reactivity in dogs with visceral leishmaniasis: correlation with T lymphocyte infiltration and with cerebrospinal fluid anti-Leishmania antibody titres. *Cell Tissue Res.* (2011) 346:293–304. doi: 10.1007/s00441-011-1290-7
 40. Headley SA, Soares IC, Graça DL. Glial Fibrillary Acidic Protein (GFAP)-immunoreactive astrocytes in dogs infected with canine distemper virus. *J Comp Pathol.* (2001) 125:90–7. doi: 10.1053/jcpa.2001.0483
 41. Lee KM, Chiu KB, Sansing HA, Didier PJ, Ficht TA, Arenas-Gamboa AM, et al. Aerosol-induced brucellosis increases TLR-2 expression and increased complexity in the microanatomy of astroglia in rhesus macaques. *Front Cell Infect Microbiol.* (2013) 3:86. doi: 10.3389/fcimb.2013.00086
 42. Bouchard PR, Weldon AD, Lewis RM, Summers BA. Uremic encephalopathy in a horse. *Vet Pathol.* (1994) 31:111–5. doi: 10.1177/030098589403100116
 43. Frye MA, Johnson JS, Traub-Dargatz JL, Savage CJ, Fettman MJ, Gould DH. Putative uremic encephalopathy in horses: five cases (1978–1998). *J Am Vet Med Assoc.* (2001) 218:560–6. doi: 10.2460/javma.2001.218.560
 44. Giannitti F, Diab SS, Pacin AM, Barrandeguy M, Larrere C, Ortega J, et al. Equine leukoencefalomalacia (ELEM) due to fumonisins B1 and B2 in Argentina. *Pesqui Vet Bras.* (2011) 31:407–12. doi: 10.1590/S0100-736X2011000500007
 45. Bandarra PM, Pavarini SP, Raymundo DL, Correa AMR, Pedroso PMO, Driemeier D. Trematode micrantha toxicity in horses in Brazil. *Equine Vet J.* (2010) 42:456–9. doi: 10.1111/j.2042-3306.2010.00035.x
 46. Jenkinson SP, Grandgirard D, Heidemann M, Tschertner A, Avondet M-A, Leib SL. Embryonic stem cell-derived neurons grown on multi-electrode arrays as a novel *in vitro* bioassay for the detection of *Clostridium botulinum* neurotoxins. *Front Pharmacol.* (2017) 8:73. doi: 10.3389/fphar.2017.00073
 47. Eid MM, El-Kowrany SI, Othman AA, El Gendy DI, Saied EM. Immunopathological changes in the brain of immunosuppressed mice

- experimentally infected with *Toxocara canis*. *Korean J Parasitol.* (2015) 53:51–8. doi: 10.3347/kjp.2015.53.1.51
48. Liao C-W, Cho W-L, Kao T-C, Su K-E, Lin Y-H, Fan C-K. Blood-brain barrier impairment with enhanced SP, NK-1R, GFAP and claudin-5 expressions in experimental cerebral toxocarosis. *Parasite Immunol.* (2008) 30:525–34. doi: 10.1111/j.1365-3024.2008.01048.x
 49. Sikasunge CS, Johansen M V., Phiri IK, Willingham AL, Leifsson PS. The immune response in *Taenia solium* neurocysticercosis in pigs is associated with astrogliosis, axonal degeneration and altered blood-brain barrier permeability. *Vet Parasitol.* (2009) 160:242–50. doi: 10.1016/j.vetpar.2008.11.015
 50. Bardina S V, Lim JK. The role of chemokines in the pathogenesis of neurotropic flaviviruses. *Immunol Res.* (2012) 54:121–32. doi: 10.1007/s12026-012-8333-3
 51. Pekny M, Pekna M. Reactive gliosis in the pathogenesis of CNS diseases. *Biochim Biophys Acta Mol Basis Dis.* (2016) 1862:483–91. doi: 10.1016/j.bbadis.2015.11.014
 52. Mayaki AM, Abdul Razak IS, Mohd Adzahan N, Mazlan M, Abdullah R. Myelopathy and reactive microgliosis and astrogliosis in equine back pain. *J Equine Vet Sci.* (2020) 90:103019. doi: 10.1016/j.jevs.2020.103019
 53. Li T, Zhang S. Microgliosis in the injured brain: infiltrating cells and reactive microglia both play a role. *Neurosci.* (2015) 22:165–70. doi: 10.1177/1073858415572079
 54. Mustafá YM, Meuren LM, Coelho SVA, de Arruda LB. Pathways exploited by flaviviruses to counteract the blood-brain barrier and invade the central nervous system. *Front Microbiol.* (2019) 10:28. doi: 10.3389/fmicb.2019.00525
 55. Cartier N, Lewis CA, Zhang R, Rossi FM V. The role of microglia in human disease: therapeutic tool or target? *Acta Neuropathol.* (2014) 128:363–80. doi: 10.1007/s00401-014-1330-y
 56. MacKay RJ, Granstrom DE, Saville WJ, Reed SM. Equine protozoal myeloencephalitis. *Vet Clin North Am Equine Pract.* (2000) 16:405–25. doi: 10.1016/S0749-0739(17)30086-X
 57. Witonsky S, Sellon DC, Dubey JP. Equine protozoal myeloencephalitis. In: Sellon DC, Long MT, editors. *Equine Infectious Diseases*. 2nd ed. Saint Louis, MO: Elsevier (2014) p. 456–67.e6.
 58. Vasconcelos RDO, Lemos KR, De Moraes JRE, Borges VP. *Halicephalobus gingivalis* (H.deletrix) in the brain of a horse. *Cienc Rural.* (2007) 37:1185–7. doi: 10.1590/S0103-84782007000400047
 59. Bassuino D, Konradt G, Cruz RAS, Silva GS, Gomes DC, Pavarini SP, et al. Characterization of spinal cord lesions in cattle and horses with rabies. *J Vet Diagn Investig.* (2016) 28:455–60. doi: 10.1177/1040638716647992
 60. Lorenzetti MP, Pereira PR, Bassuino DM, Konradt G, Panziera W, Bianchi M V, et al. Neurotoxicosis in horses associated with consumption of *Trema micrantha*. *Equine Vet J.* (2018) 50:192–5. doi: 10.1111/evj.12741
 61. Bielefeldt-Ohmann H, Bosco-Lauth A, Hartwig A-E, Uddin MJ, Barcelon J, Suen WW, et al. Characterization of non-lethal West Nile Virus (WNV) infection in horses: subclinical pathology and innate immune response. *Microb Pathog.* (2017) 103:71–9. doi: 10.1016/j.micpath.2016.12.018
 62. Cantile C, Piero F del, di Guardo G, Arispici M. Pathologic and immunohistochemical findings in naturally occurring west nile virus infection in horses. *Vet Pathol.* (2001) 38:414–21. doi: 10.1354/vp.38-4-414
 63. Eydal M, Bambir SH, Sigurdarson S, Gunnarsson E, Svansson V, Fridriksson S, et al. Fatal infection in two Icelandic stallions caused by *Halicephalobus gingivalis* (Nematoda: Rhabditida). *Vet Parasitol.* (2012) 186:523–7. doi: 10.1016/j.vetpar.2011.11.024
 64. Wierzbza-Bobrowicz T, Gwiazda E, Kosno-Kruszewska E, Lewandowska E, Lechowicz W, Bertrand E, et al. Morphological analysis of active microglia-rod and ramified microglia in human brains affected by some neurological diseases (SSPE, Alzheimer's disease and Wilson's disease). *Folia Neuropathol.* (2002) 40:125–31.
 65. Fumagalli S, Perego C, Pischiutta F, Zanier ER, De Simoni M-G. The ischemic environment drives microglia and macrophage function. *Front Neurol.* (2015) 6:81. doi: 10.3389/fneur.2015.00081

Conflict of Interest: The authors declare that the research was conducted in the absence of any commercial or financial relationships that could be construed as a potential conflict of interest.

Copyright © 2021 Boos, Failing, Colodel, Driemeier, Castro, Bassuino, Diomedes Barbosa and Herden. This is an open-access article distributed under the terms of the Creative Commons Attribution License (CC BY). The use, distribution or reproduction in other forums is permitted, provided the original author(s) and the copyright owner(s) are credited and that the original publication in this journal is cited, in accordance with accepted academic practice. No use, distribution or reproduction is permitted which does not comply with these terms.